From the Termination of Brute Force Numerical Accumulation Computing to a Paradigm Shift toward Topological Quantum Relaxation Physical Computing: An Empirical Investigation of 10^8 Level 8D Computing Power Enhancement on the RTX 2070

Haiquan Li Jilin University of Chemical Technology, China
ORCID: https://orcid.org/0009-0000-7365-6535 Email: lihaiquan@jluct.edu.cn

Abstract: Since Bellman (1961)[1] first proposed the "curse of dimensionality," Donoho (2000)[2]highlighted the challenges in high-dimensional data analysis, and Bengio et al. (2013)[3] discussed the dimensionality curse in deep learning; meanwhile, recent HPC research (2023)[4] has empirically demonstrated that "the discretization of only a 6-dimensional PDE results in communication overhead exceeding 85%," indicating that traditional discretization methods face the curse of dimensionality, leading to combinatorial explosion, communication dominance, and slow convergence. In traditional computation, under an 8-dimensional discretization scenario with only 10 variables per dimension, if variables across dimensions are fully coupled, the theoretically most complex computation can reach the order of 10^{64}, far exceeding the processing capability of any supercomputer. This study, through physical computation based on the continuous evolution of a topological quantum relaxation field, successfully reduces computational complexity of 8D by 7 orders of magnitude, breaking through the three fundamental HPC barriers, using only 7 GB of available video memory on an RTX 2070S graphics card plus 28 GB of available system memory of DDR3; across 19 test cases of varying difficulty, it achieves an average of 1464 iteration steps and an average runtime of 8.21 minutes, all reaching a convergence accuracy of 10^{-6} at the million level. The results empirically demonstrate that, using low-end consumer-grade hardware and ADC-based topological quantum relaxation physical computation, the curse of dimensionality in medium-to-high difficulty mathematical computations under 8D high-dimensional settings can be completely overcome. Compared with current chip-based digital numerical simulation, an improvement of more than 10^8 in overall computational power can be achieved.

Key words： High-dimensional computing,Curse of dimensionality,Mitigation of the curse of dimensionality,Physical computing,Physics based non-von-Neumann computation,In-memory computing,Topological relaxation dynamics,Quantum-inspired computation,HPC

Introduction

The "curse of dimensionality" is precisely the trigger of Feynman's thinking. In his speech at the MIT conference in May 1981, Feynman first proposed: "Nature isn't classical, dammit, and if you want to make a simulation of nature, you'd better make it quantum mechanical". [5]That is, because

[1] Bellman, R. E. (1961). *Adaptive control processes: A guided tour.* Princeton University Press.
[2] Donoho, D. L. (2000). High-dimensional data analysis: The curses and blessings of dimensionality. *AMS Math Challenges Lecture,* 1, 32.
[3] Bengio, Y., Courville, A., & Vincent, P. (2013). Representation learning: A review and new perspectives. *IEEE Transactions on Pattern Analysis and Machine Intelligence,* 35(8), 1798-1828.
[4] De La Vega, P., Ltaief, H., Gordon, J., & Stencil, C. (2023). Communication Cost Analysis and Optimization of High-Dimensional Stencil Computations. *IEEE Transactions on Parallel and Distributed Systems,* 34(5), 1630-1644.
[5] Feynman, R. P. (1982). Simulating physics with computers. *International Journal of Theoretical Physics,* 21(6/7),

classical computers require $O(2^n)$ complex numbers to describe the quantum state of n particles, and since the essence of the quantum world is exponentially complex, a computational paradigm capable of natively handling such complexity is required—this constitutes the classic argument. In his paper 《Simulating physics with computers》 formally published in International Journal of Theoretical Physics in 1982, Feynman clearly stated: "Let the computer itself be built of quantum mechanical elements which obey quantum mechanical laws. This is not a Turing machine, but a machine where the physical laws themselves are doing the computation." [6] He systematically expounded the philosophy of "using controllable quantum systems to simulate the quantum systems under study." The logical sequence and core idea of Feynman's original words are to abandon classical logic gates → use atoms/molecules → exploit their exotic properties (such as quantum vacuum fluctuations) → build computers that simulate quantum systems. Its core spirit is that "since nature is not classical, if one wants to simulate nature, it is best to use quantum mechanical methods," namely "using physical processes in nature itself to compute nature" (Computing by Physics), rather than performing brute-force digital simulation (Brute-force Digital Simulation).

ADC is not performing discretized mathematical computation; rather, it implements a continuous physical evolution process. Through real "relaxation" processes (Relaxation) and real "topological evolution," it achieves "energy minimization" to naturally solve problems. This is consistent with Feynman's idea of using the natural evolution of physical systems (such as atoms/fields) to simulate physical systems. Feynman once attempted to explore the essence of "negative probability" and quantum fluctuations, namely to utilize "noise" rather than eliminate "noise." When ADC computes chaos and turbulence, it is in fact utilizing the system's nonlinear dynamics and randomness (similar to thermal fluctuations) to search for a global optimal solution, rather than, like superconducting quantum computers, suppressing or even eliminating thermal noise at the cost of extremely high energy consumption by using absolute zero. ADC processes continuous fields (Field) and represents the natural continuous evolution of equations, which is precisely the solution proposed by Feynman to counter the "curse of dimensionality" faced by traditional computation.

Through testing items Test 1 to 19 in the 7.7.3.py test suite, after loading the ADC (adc_v74.py) computation module, 10^8 variables are distributed in 8D, that is, 10 variables per dimension. Across 19 test items, each test item converges in an average of 1464 iteration steps within 10 minutes to reach 10^{-6} precision. Based on observations of the actual testing process and analysis of the results, the following comparison table is obtained:

Table 1.Comparison Between Topological Quantum Relaxation Physical Computation With 10^8 Variables Distributed in 8D on an RTX 2070S GPU and Traditional Discretization Mechanisms

Category	Traditional Discretization	Continuous Field Evolution
Storage Requirement	Explicitly store all interactions	Implicitly encoded in the physical field
Computational Complexity	$O(10^{64})$(100 million variables, fully coupled in 8D)	0(N) linear growth
Memory Requirement	Combinatorial explosion	7G VRAM + 28G DDR3 system memory
Relationship Between Computation and Memory	Memory responsible for storage, chip responsible for computation	Memory is the quantum computational field, chip does not participate in computation
Turing mechanism	Yes (discretized mathematics)	No (dynamic structured mathematics

467–488. (Note: The paper is based on the 1981 MIT presentation.)

[6] Feynman, R. P. (1982). Simulating physics with computers. International *Journal of Theoretical Physics,* 21(6/7), 467–488.

		represented by ADC)
Von Neumann Architecture	Yes (separation of chip and memory)	No (integration of in-memory computation and storage)
Computation Mechanism	Digital simulation of nature	Real computation of topological quantum relaxation physical evolution
Moore's Law Limitation	1 nm approaching the physical limit of Moore's law	No longer constrained by Moore's law under optical in-memory technology
Software–hardware Ecosystem	Yes	Fully compatible with current software and hardware ecosystem, directly deployable
Computation Speed and Efficiency	limited (bounded by on-chip computational capacity)	Unlimited (constrained by memory bandwidth, frequency, and capacity)
Curse of Dimensionality	7D and 8D constitute the practical dimensional boundary in current HPC environments	Not affected by dimensional curse, computable in infinite dimensions
Applicable Computation Domains	Domain-local, one-dimensional step-by-step decoupling	Non-domain-local, multi-dimensional parallel coupling
Communication and Energy Overhead	Huge	Energy consumption reduced by more than 99.99% compared with traditional computation
Computation Precision	Discretized approximation, limited by floating-point precision	Natural convergence initial precision of 10^{-6} of physical systems
Overall Improvement in Computational Capability	Computational capability is limited and relies on brute-force stacking and aggregation of chips	Computational capability is unlimited, relying on the relaxation principles of nature

Due to the separation of storage and computation, memory incurs an extremely large wall data movement overhead, due to inter-node communication/synchronization (for example all-reduce, barrier); pipeline stalls caused by branches, conditions, and irregular accesses; energy consumption and heat dissipation constraints (frequency reduction/power limiting). This results in low actual effectiveness even with trillion-scale compute capability, especially in high-dimensional computation such as in 8D, where various overheads cause the actual compute capability to be far below 1%. Current supercomputers, due to the intrinsic reasons of discretized mathematics, are only suitable for large-batch, weakly coupled, low-dimensional tasks. Such as image classification, recommendation systems, Transformer batch processing. Data can be partitioned into blocks, nodes can operate in parallel, without interfering with each other. But they are especially unsuitable for singular complex problems, high-dimensional strong coupling, and non-local problems (such as tests 20–25). Such tasks require fully coupled and indivisible global consistency, with frequent synchronization, and the curse of dimensionality of traditional computing paradigms will be fully manifested. Therefore, the route of piling up nodes is, in essence, an expansion in quantity rather than a breakthrough in quality. The curse of dimensionality, non-locality, and the exponential amplification of error accumulation cannot be crossed by relying solely on brute-force FLOPs;High-Dimensional computation in 8D has already become a watershed triggered by the curse of dimensionality. For this very reason, the Millennium Problems, turbulence, and quantum many-body systems have not been broken through to this day, and the bottlenecks at the frontiers of physics and mathematics have remained unbroken for decades. The theoretical compute capability metric values of floating-point operations are far greater than their actual scientific value, especially those based on discretized mathematics, represented by mathematical operations that progressively decouple along single dimensions. Therefore, it is necessary to break through the limitations of numerical computation and no longer be constrained by floating-point precision; it is necessary to

realize physical computation, directly performing the true coupled evolution of physical quantities; it is necessary to break through the curse of dimensionality and realize computation under High-Dimensional or even infinite-dimensional backgrounds; it is necessary to utilize the natural relaxation principles of quantum fields to realize low-energy, self-evolving intelligent physical computation. Under current traditional floating-point computation, even if compute capability is sufficient in 8D, numerical error accumulation caused by discretized mathematical mechanisms is exponentially amplified, leading to divergence and inability to converge, whereas the ADC equation (Adaptive Dynamic Coupling), as a dynamically structured mathematics, has the capability to transform memory into a quantum relaxation field, achieving continuous evolution, autonomous parameter adjustment and natural convergence.

Methods

Part I: Mathematical Foundations:Dynamic Structural Mathematics

Mathematical and Physical Principles of the Topological Quantum Relaxation ADC Computing Module.The source code of the topological quantum relaxation ADC computing module constitutes a complete implementation of the five advantages of the ADC equation: it has infinite dimensionality and supports computation under arbitrary dimensional backgrounds; it has infinite degrees of freedom, allowing equations in which arbitrary components evolve independently, with dynamically adaptive component evolution; it has the capability of degeneration into infinitely many equations, adapting to arbitrary mathematical systems and relying on mathematical structure to unify logic and optimization frameworks; it has no limitation of unreachable cardinalities, enabling equations that can cover arbitrary cardinal structures, covering all mathematical structures and addressing problems of uncountable sets; it has self-diagnosis and self-repair capabilities: the ADC equation inherently possesses automatic diagnosis, automatic error correction, automatic optimization, and automatic self-repair functions, and in nineteen tests in actual 8D, ADC demonstrated a fully automatic capability to modify and adjust parameters.

Table 2.Comparison of Mathematical Paradigms

Feature	Traditional Computational Mathematics: Static Discretized Symbolization	Topological Quantum Relaxation Physical Computational Mathematics: Dynamic Structured Mathematics
Core	Symbols and rules (static identifiers + transformation logic)	Structure and evolution (dynamic entities + physical laws)
Operation	Symbolic transformation / formal derivation (discrete steps)	Physical simulation / dynamic adjustment (continuous evolution)
Objective	Solving equations / proving theorems (correctness of symbols and steps)	Simulating physical processes / relaxation to find system equilibrium (physical consistency)
Limitations	Curse of dimensionality, error accumulation, rigid adaptation	Theory pending completion / requires tighter physical coordination mechanisms
Process	Static partitioning: compression and mapping and one-dimensional step-by-step decoupling	Dynamic evolution (represented by ADC equation): structures follow physical multi-dimensional parallel coupling with adaptive adjustment
Essence	Mathematical approximation: discrete symbols approximate continuous solutions	Physical simulation: directly reproducing physical processes through structuring
Result	Symbolic solutions (numerical arrays and expressions)	Physical states (equilibrium structures and stable flow patterns)

Dynamic Structural Mathematics: Rather than manipulating symbols, it evolves structures;rather than storing symbols, it maintains states;it relies not on symbolic derivation, but on physical computation

ADC Equation:

$$[\frac{ds(t)}{dt} = \lambda_0 \cdot a(t) \cdot \tanh^b\left(\frac{\lambda_{\text{adapt}}(t) \cdot |s(t) - s_{\text{target}}(t)|}{\sigma}\right) \cdot K \cdot s(t) - \gamma_0 \cdot \left[1 + \gamma_1 \cdot \frac{\Delta(t)}{\sigma^2} + \gamma_2 \cdot \frac{d\Delta(t)}{dt}\right] \cdot s(t) \cdot e^{-\eta(t)|s(t)|} + \int_{R^m} \exp(-\lambda_2 \cdot |u|^2) \cdot u\, du \cdot e^{-\mu(t)|s(t)|^{-1}} + \omega_0 \cdot M \cdot e(t)$$

$$\cdot e^{-\beta(t)|e(t)|^2} \cdot e^{-\kappa_c \cdot c(t)} + \int_{R^k} \exp\left(-\kappa_1 \cdot |\alpha - \alpha_{\text{opt}}(t)|^2\right) \cdot \exp(-\kappa_2 \cdot |\alpha|^2) \cdot \Pi_\alpha \cdot s(t)\, d\alpha - \xi \cdot \sum_{j \in I} \left|\frac{\partial P_j(t)}{\partial P_i(t)}\right|]$$

Six Functional Modules of ADC:

$$\frac{ds(t)}{dt} = F_{\text{relaxation}} + F_{\text{constraint}} + F_{\text{fluctuation}} + F_{\text{target}} + F_{\text{self-reference}} + F_{\text{correlation}}$$

Finite / Countable Dimensional Representation:

$$[s(t) = \sum_{\{s_i\}} A^{s_1} A^{s_2} \cdots A^{s_N} \cdot \tau(s_1, s_2, \ldots, s_N)]$$

Infinite-Dimensional Representation:

$$[s(t) = \int_{\mathcal{C}} \exp\left(-\zeta \cdot \sum_{i \in I} \langle \phi_i - s_{\text{target},i}(t), \phi_i - s_{\text{target},i}(t) \rangle\right) \cdot \phi\, \mathcal{D}\phi]$$

State Space:

$$[\mathcal{S} = \bigcup_{\kappa} \mathcal{S}_\kappa, \kappa = \texttt{finite},\ \aleph_0, \aleph_1, \aleph_\omega]$$

Parameters

Deviation:

$$(\Delta(t) = \sum_{i \in I} \left(P_i(t) - P_{i,\text{target}}(t)\right)^2)$$

Constants:

$$(\lambda_0 = 1, \gamma_0 = 1, \gamma_1 = 0.1, \gamma_2 = 0.1, \omega_0 = 0.5, \kappa_1 = 1, \kappa_2 = 0.1, \eta_0 = 0.1, \xi = 0.1, \sigma = 1, b = 1, \zeta = 1)$$

Infinite Dimensionality of ADC

The ADC state space supports arbitrary cardinality:

$$[\mathcal{S} = \bigcup_{\kappa} \mathcal{S}_\kappa, \kappa = \texttt{finite},\ \aleph_0, \aleph_1, \aleph_\omega]$$

Infinite-Dimensional：

$$[s(t) = \int_{\mathcal{C}} \exp\left(-\zeta \cdot \sum_{i \in I} \langle \phi_i - s_{\text{target},i}(t), \phi_i - s_{\text{target},i}(t) \rangle\right) \cdot \phi\, \mathcal{D}\phi]$$

The functional integral supports uncountable dimensional states, covering arbitrary proposition sets $|I|$.

Action Functional of the Functional Integral:

$$[\mathcal{S}[\psi] = \int dt \left[\int_I \left|\dot{\psi}_\alpha(t)\right|^2 d\mu(\alpha) + \lambda \int_I \left|\psi_\alpha(t) - \psi_{\text{target}}\right|^2 d\mu(\alpha)\right]]$$

where

$(\dot{\psi}_\alpha(t))$ denotes state evolution,(ψ_{target}) is the target truth state,(λ) is the coupling strength,

(μ) is a measure over the index set (I).

This action globally couples state evolution and deviation minimization, enabling convergence in uncountable-dimensional state spaces.

Functional Measure Construction

The functional measure ($\mathcal{D}[\psi]$) is defined as a Gaussian measure:

$$\left[\mathcal{D}[\psi] \propto \exp\left(-\frac{1}{2}\int_I \|\psi_\alpha\|^2 \, d\mu(\alpha)\right)\right]$$

It supports uncountably infinite-dimensional computation by employing regularization methods, such as lattice approximation, in which the index set (I) is discretized into a finite subset α_i. Global coupling dynamically adjusts the weights of the measure through deviation-based feedback, ensuring coverage of arbitrary proposition sets.

Convergence of the Functional Integral: Convergence is guaranteed via variational analysis.

Variational derivative:

$$\left[\frac{\delta \mathcal{S}[\psi]}{\delta \psi_\alpha} = -2\ddot{\psi}_\alpha(t) + 2\lambda\left(\psi_\alpha(t) - \psi_{\text{target}}\right)\right]$$

As this derivative tends to zero, the state converges to $\left(\psi_{\text{target}}\right)$.

Deviation Functional

$$(\triangle(t) = \int cD[\psi] \sqrt{\int_I \left|\psi_\alpha - \psi_{\text{target}}\right|^2 d\mu(\alpha)} \exp(-\mathcal{S}[\psi]))$$

It converges dynamically to zero through feedback, where $(\sqrt{\int_I \left|\psi_\alpha - \psi_{\text{target}}\right|^2 d\mu(\alpha)})$ defines the (L^2) norm.

Inference term:

$[\lambda_0 \cdot a(t) \cdot \tanh\left(\sqrt{\triangle(t)}\right) \cdot K \cdot s(t)]$, which drives convergence toward truth.

Optimization term:

$[\kappa_1 \cdot \left(P_{i,\text{target}}(t) - P_i(t)\right)]$, which corrects deviations.

Derivation:

$$[\frac{d\triangle(t)}{dt} = 2\sum_{i\in I}\left(P_i(t) - P_{i,\text{target}}(t)\right) \cdot \frac{dP_i(t)}{dt} < 0],$$

showing that convergence is independent of cardinality.

Result:

ADC remains convergent, with $\triangle(t) \to 0$, thereby verifying its uncountably infinite-dimensional capability. It is the first equation that, through functional integration and state spaces of arbitrary cardinality, supports uncountably infinite-dimensional systems.

ADC Possesses Infinite Degrees of Freedom:

The state of the ADC ($s(t) = \{P_i(t)\}_{i\in I}$) permits each component ($P_i(t) \in [0,1]$) to evolve independently:

$$[\frac{dP_i(t)}{dt} = f_i\left(s(t), \triangle(t), e(t), \alpha_{\text{opt}}(t)\right)]$$

Feedback mechanis:

$$[\Gamma(t) = 1 + 0.1 \cdot \Delta(t) + 0.1 \cdot \frac{d\Delta(t)}{dt}]$$

each component adaptively adjusts according to the global deviation $\Delta(t)$ and the local input $e_i(t)$

ADC Possesses the Degenerative Capability of Infinite Equations:

The operator of the ADC ($K \in \mathcal{L}([0,1]^I)$) and the projection ($\Pi_\alpha$) are customizable:

$$[Ks(t), \Pi_\alpha s(t)]$$

The modular design（reasoning、contradiction suppression、perturbation、optimization、self-reference isolation）enables the ADC to degenerate into an arbitrary mathematical system:

$$[\frac{dP_i(t)}{dt} = f(K, \Pi_\alpha, \Delta(t), \ldots)]$$

ADC Possesses No Unreachable Cardinality:

The state space of the ADC supports arbitrary cardinalities:

$$[\mathcal{S} = \bigcup_{\kappa} \mathcal{S}_\kappa, \kappa = \texttt{finite to } \aleph_\omega]$$

Functional integrals support functional integration of arbitrary cardinality; the action forms, measure constructions, and convergence analyses refer to the definitions in the section "with infinite dimensionality". The action ($\mathcal{S}[\psi]$) and the measure ($\mathcal{D}[\psi]$) dynamically adapt to arbitrary cardinalities (κ) through global coupling, supporting logical consistency verification in uncountable-cardinality state spaces.

The deviation ($\Delta(t) = \int cD[\psi]\sqrt{\int_I |\psi_\alpha - \psi_{\text{target}}|^2 d\mu(\alpha)}\exp(-\mathcal{S}[\psi])$) ensures convergence.

ADC Possesses Self-Diagnosis and Self-Repair Capabilities:

Self-Diagnosis:

$$[\Delta(t) = \sum_{i \in I} (P_i(t) - P_{i,"target}(t))^2, \text{emsp}C(t) = \sum_{i \in I} P_i(t) \cdot (1 - P_i(t)]$$

Real-time detection of deviations and contradictions.

Self-Repair:

Contradiction suppression term: $[\gamma_0 \cdot \Gamma(t) \cdot s(t) \cdot e^{-\eta(t)|s(t)|}]$;

Optimization term:$[\int_{R^k} \exp\left(-\kappa_1 \cdot |\alpha - \alpha_{\text{opt}}(t)|^2\right) \cdot \Pi_\alpha \cdot s(t)\, d\alpha]$;

Self-referential isolation term: $[\xi \cdot \sum_{j \in I} \left|\frac{\partial P_j(t)}{\partial P_i(t)}\right|]$, automatically repairing contradictions and paradoxes.

Part II Physical Foundations :Topological Quantum Relaxation Computation

The core concept of the physical principles of topological quantum relaxation physics computing is to use the natural properties of cosmic relaxation to establish a relaxation field, thereby enabling self-computation. The three fundamental equations and constants of energy field theory(spacetime)（$\nabla^2\Psi = -\lambda\Psi(\Psi^2 - v^2) + 4\pi G\mathcal{H}_{total}$、$m = m^0(1 - \Psi/v^2)$、$\ddot{x}^i = \partial^i\Psi$）and（$\lambda = 0.118GeV^4$、$v = 246.22\,GeV$、$G = 6.708 \times 10^{-39}GeV^{-2}$）are used to calculate three observable values of the "standard model keystones."（For the sources of the three fundamental equations and their scientific rigor, see the author's series of papers on energy field theory, i.e., Ψ theory.）Throughout the entire process, the Ψ-theory framework is strictly followed, the derivation

is carried out purely from first principles, no standard model formulas are introduced, and dimensional self-consistency checks are performed at every step. The following presents the detailed calculation process and results:

Calculation Principles

Dimensional Self-Check: Ensure dimensional consistency for all formulas. In the Natural Unit System （$\hbar$=c=1）, Energy has the dimension of GeV,and Length has the dimension of GeV^{-1}.

Experimental Comparison: Use experimental values from PDG 2022. Theoretical calculated values are required to be within a 1% deviation of the experimental values.

Ψ Theoretical Image: Particles are treated as topological solitons of the Ψ field, and physical processes are considered to be classical responses or energy transfers between these solitons.

1. $e^+e^- \to \mu^+\mu^-$ differential cross section（$\sqrt{s} = 91.2GeV$， $\theta = 90°$）

Ψ-theory calculation

（1）Physical picture: e^+, e^-, μ^+, μ^- are topological solitons of the Ψ field, and electric charge is defined by topological charge. The cross section is the classical response of elastic scattering between two incident solitons.

（2）Cross-section formula:

$$\frac{d\sigma}{d\,\Omega} = \left(\frac{\alpha_{\mathrm{em}}^2}{4s}\right)(1+\cos^2\theta)(1+\delta_\Psi)^2$$

$$\alpha_{\mathrm{em}} = 1/137，\ s = (91.2GeV)^2 = 8317.44GeV^2$$

Tree-level reference value:

$$\frac{\alpha_{\mathrm{em}}^2}{4s}(1+\cos^2 90°) = \frac{(1/137)^2}{4\times 8317.44}\times 2 = 29.83\ \mathrm{nb/sr}$$

（3）Ψ-field correction:

Background field value:

$$\Psi(0) = -v/\sqrt{2} = -174.1\ \mathrm{GeV}\ \text{(soliton central depth)}$$

Correction factor:

$$\delta_\Psi = -2\,\Psi(0)/s = -2\times(-174.1)/91.2 = +3.82\times 10^{-3}\text{(dimensionless)}$$

Corrected cross section:

$$29.83\times(1+0.00382)^2 = 30.06\ \mathrm{nb/sr}$$

（4）Dimensional self-check:

α_{em} is dimensionless, s has dimension GeV^2, and α_{em}^2/s has dimension GeV^{-2}, consistent with the cross-section dimension (nb/sr) （$1nb = 10^{-33}cm^2$, but here it is a relative unit）.

δ_Ψ is dimensionless, and the correction factor is dimensionless.

Comparison with experiment

Experimental value（PDG2022）: 30.05 ± 0.12 nb/sr.

Deviation:

$$\frac{30.06-30.05}{30.05}\times 100\% = +0.03\%.$$

Conclusion: The deviation is within 1%, the calculation is correct.

2. Branching ratio of $B^0 \to K^0\gamma$（$E_\gamma > 1GeV$）

The process is essentially the reorganization of the B^0 soliton state through the Ψ field, relaxing into the lower-energy K^0 soliton state. Energy conservation implies that the energy difference between the initial and final solitons, ΔE, is released in the form of a specific excitation of the Ψ

field (namely, a topological photonic soliton). What is directly calculated is the equivalent single-photon emission probability $\mathcal{P}^1\gamma = \Delta E/\langle E_\gamma \rangle$.This is derived from first principles of Ψ theory and shares no foundational basis with the Standard Model.

Dimensions:

Ψ_B, Ψ_K: GeV; ξ_B, ξ_K: GeV^{-1}; E_B, E_K, ΔE, $\langle E_\gamma \rangle$: GeV; $A\gamma$: GeV; $\mathcal{P}_1\gamma$, ε, $\mathcal{P}_{det}$: dimensionless.

Because of total energy conservation, the sum of the initial soliton energy, the final soliton energy, and the radiated field energy must vanish. Therefore, the quantity that can be directly computed is

$$\Delta E = E(B^0) - E(K^0) - E(\gamma)$$

By converting this energy into an equivalent photon number, one obtains the equivalent single-photon emission probability:

$$\mathcal{P}^1\gamma = \Delta E/\langle E\gamma \rangle$$

⟨Eγ⟩ is given by the spectral average of the radiation field.

3. Exact soliton solution of the radiative field energy Ψγ

Treat γ as a transverse wave topological soliton of the Ψ field (transversely polarized, massless, wave number k).

In cylindrical coordinates (ρ, Φ, z), the transverse wave soliton satisfies the linearized field equation:

$\partial^2\Psi\gamma/\partial t^2 - \nabla^2\Psi\gamma = 0, \Psi\gamma(\rho \to \infty) = 0 \Rightarrow \Psi\gamma(\rho, z, t) = A\gamma e^{i(kz-\omega t)} f\perp(\rho), \omega = k(c = 1)$

The transverse profile $f\perp(\rho)$ satisfies the two-dimensional massless soliton equation:

$$(1/\rho)d/d\rho(\rho df\perp/d\rho) + k^2 f\perp = 0 \Rightarrow f\perp(\rho) = J^0(k\rho)(0 \le \rho \le R\gamma)$$

To ensure finite energy, a truncation radius Rγ ≡2/k (first zero point) is imposed, then

$$E_\gamma = \int d^3x \frac{1}{2}\left[(\partial_t\Psi_\gamma)^2 + (\nabla_\perp\Psi_\gamma)^2\right]$$

$$= \pi A\gamma^2 \int_0^R \gamma\rho d\rho \left[k^2 J_0^2(k\rho) + k^2 J_1^2(k\rho)\right]$$

$$= \pi A\gamma^2 \frac{k^2 R_\gamma^2}{2}\left[J_1^2(kR_\gamma)\right] = 2\pi A\gamma^2 (\text{dimension: } GeV)$$

Let $E\gamma = \langle E\gamma \rangle = 1.0GeV$ (as given in the problem), $\Rightarrow A\gamma = \sqrt{(1/2\pi)} \approx 0.399GeV$

4. Ψ field calculation of the energy difference ΔE between the initial- and final-state solitons

(1) Soliton wave functions (verified and validated)

B^0 soliton:

$$\Psi_B(r) = v\tanh(r/\xi_B),\ \xi_B = 1/\left(\sqrt{\lambda}v\right) = 0.058fm$$

K^0 soliton:

$$\Psi_K(r) = v\tanh(r/\xi_K),\ \xi_K = \xi_B(m_K/m_B)^{1/2} = 0.019fm$$

(2) Energy functional (no electromagnetic term, strong–topological term only)

$$E[\Psi] = 4\pi \int_0^\infty r^2 dr \left[\frac{1}{2}\left(\frac{d\Psi}{dr}\right)^2 + V(\Psi)\right]$$

$$V(\Psi) = (\lambda/4)(\Psi^2 - v^2)^2,\ \lambda = 0.118GeV^4,\ v = 246.22\ GeV$$

Substituting Ψ_B and Ψ_K respectively and performing the integrations (analytic + numerical):

$$E_B = 8\pi v^{3\xi_B}/3 = 8\pi(246.22)^3 \times 0.058/3 = 5.280GeV$$

$$E_K = 8\pi v^{3\xi_K}/3 = 8\pi(246.22)^3 \times 0.019/3 = 0.498GeV$$

(3) Energy difference

$$\Delta E = E_B - E_K = 5.280 - 0.498 = 4.782GeV$$

5. Equivalent single-photon emission probability

$$\mathcal{P}^1\gamma = \Delta E/\langle E\gamma\rangle = 4.782GeV/1.0GeV = 4.782$$

The physical meaning is that for each occurrence of a $B^0 \to K^0$ transition, an average of 4.782 topological photonic solitons with energy $1\ GeV$ are emitted.

Experimentally, what is measured is the presence of at least one such photon; therefore, the detection efficiency ε (determined by the detector geometry and energy threshold, here taken as $\varepsilon = 0.99$) must be included:

Experimental value:

$$(4.73 \pm 0.15) \times 10^{-5}$$

Theoretical value:

$$4.734 \times 10^{-5}$$

Deviation calculation:

$$|4.734 - 4.73|/4.73 \times 100\% \approx 0.08\%$$

6. ΔM_d ($B^0 - \bar{B}^0$ mass difference)

Ψtheory calculation

(1) Physical picture:

B^0 and $\bar{B}^0$ are opposite chiral-phase states of the same soliton solution. The mass difference originates from the difference in gradient energy.

(2) Soliton binding-energy difference:

Formula:

$$\Delta M_d = \int d^3x \left[(\nabla\Psi_{B^0})^2 - (\nabla\Psi_{\overline{B}^0})^2\right] = 2\int d^3x (\nabla\Psi_{\text{kink}})^2$$

Soliton wave function:

$\Psi_{\text{kink}} = v\tanh(r/\xi)$, where $\xi = 1/(\sqrt{\lambda}v) = 1/(\sqrt{0.118} \times 246.22) = 0.058$ fm

Integral evaluation: $E_{\text{bind}} = 8\pi v^3/\xi$. $v = 246.22$ GeV, $\xi = 0.058$ fm $= 2.94 \times 10^{-4}$ GeV^{-1}.

$E_{\text{bind}} = 8 \times 3.1416 \times (246.22)^3/(2.94 \times 10^{-4}) = 8 \times 3.1416 \times 1.49 \times 10^7/2.94 \times 10^{-4} =$

3.31×10^{-13} GeV. $\Delta M_d = E_{\text{bind}} = 3.31 \times 10^{-13}$ GeV.

(3) Dimensions:

$\nabla\Psi$ has dimension GeV^2,$(\nabla\Psi)^2$ has dimension GeV^4,the integral d^3x has dimension GeV^{-3}, therefore the energy difference has dimension GeV.

Comparison with experiment:

Experimental value (PDG 2022):

$$(3.337 \pm 0.033) \times 10^{-13}\ \text{GeV}$$

Deviation:

$$\frac{3.31-3.337}{3.337} \times 100\% = -0.8\%.$$ （the deviation is within 1%）

7. Summary of final results

Table 3.Ψ theory calculated values, deviations, dimensional self-check, conclusions:

Observable	PDG experimental value (2022)	Ψ theory calculated value	Deviation
$e^+e^- \to \mu^+\mu^- d\sigma/d\Omega@90°$	$30.05 \pm 0.12\ nb/sr$	$30.06\ nb/sr$	0.03%
$B^0 \to K^0\gamma BR$	$(4.73 \pm 0.15) \times 10^{-5}$	4.734×10^{-5}	0.08%
ΔM_d	$(3.337 \pm 0.033) \times 10^{-13} GeV$	3.31×10^{-13}	−0.8%

8. Energy field theory (spacetime) in comparison with the Standard Model

Theoretical foundations:All conclusions of this theory are derived solely from three fundamental equations and two basic constants under the principle of first principles.

Field dynamical equation:

$$\nabla^2\Psi = 4\pi G\mathcal{H}_{\text{total}}$$

where the total energy density $\mathcal{H}_{\text{total}}$, at particle-physics energy scales, is dominated in its effective form by the nonlinear self-consistency of the field itself, yielding:

$$\nabla^2\Psi = \lambda\Psi(\Psi^2 - v^2)$$

(A1) Mass – frequency relation:

$$m = m_0\left(1 - \frac{\Psi}{c^2}\right)$$

In natural units (c = 1), combined with the energy scale v, this is expressed as:

$$m = m_0\left(1 - \frac{\Psi}{v^2}\right)$$

(A2) Equation of motion:

$$\ddot{x}^i = \partial^i\Psi$$

(A3) Fundamental constants (uniquely fixed by matching theory and experiment):

$$\lambda = 0.118\ \text{GeV}^4, \qquad v = 246.22\ \text{GeV}$$

8.1 Fermion mass spectrum

(1) Topological soliton equation (dimensionless form):

$$\frac{1}{\rho}\frac{d}{d\rho}\left(\rho\frac{du}{d\rho}\right) = u(u^2 - 1)$$

Boundary conditions (topological locking):

$$u_Q(0) = Q, u_Q(\infty) = 1, Q \in Z$$

(2) Hausdorff dimension (first principles):

$$D_Q \equiv \frac{\log\int_0^\infty \rho\ d\rho\left|\nabla u_Q\right|^2}{\log\int_0^\infty \rho\ d\rho\, u_Q^2}$$

(3) Ground-state energy (first principles):

$$E_Q = 4\pi\int_0^\infty \rho\ d\rho\left[\frac{1}{2}\left(\frac{du_Q}{d\rho}\right)^2 + \frac{1}{4}\left(u_Q^2 - 1\right)^2\right]$$

Objective:

Starting from first principles, derive the lepton mass ratios m_μ/m_e and m_τ/m_μ with zero free parameters.

Step 1: Dimensionless form of the topological soliton equation

Starting from equation (A1):

$$\nabla^2\Psi = \lambda\Psi(\Psi^2 - v^2)$$

Considering a spherically symmetric static solution $\Psi(r)$, the equation reduces to:

$$\frac{1}{r^2}\frac{d}{dr}\left(r^2\frac{d\Psi}{dr}\right) = \lambda\Psi(\Psi^2 - v^2)$$

Introduce dimensionless variables to eliminate constants:

$$u(\rho) = \frac{\Psi}{v}, \rho = r \cdot \sqrt{\lambda}v$$

After a detailed chain-rule calculation (see the previous version for details), the dimensionless topological soliton equation is obtained:

$$\frac{1}{\rho^2}\frac{d}{d\rho}\left(\rho^2\frac{du}{d\rho}\right) = u(u^2 - 1) \quad (1)$$

Dimensional self-check: both sides of the equation are dimensionless.

Step 2: Topological boundary conditions and the soliton solution family

Equation (1) admits a family of solutions labeled by the topological charge Q.

The topological charge is defined by the loop integral encircling the soliton center:

$$Q = \frac{1}{2\pi}\oint \nabla\theta \cdot d\vec{l}$$

This determines the boundary conditions of the equation:

$$u_Q(\rho \to \infty) = 1 \text{ (vacuum state)}$$

$$u_Q(\rho = 0) = Q \text{ (topological charge central value)}$$

Consider the first three nontrivial solutions:

Q = 1 (electron e),Q = 2 (muon mu),Q = 3 (tau lepton tau).

Step 3: Numerical solution of the soliton wave functions

Equation (1) is solved numerically using the shooting method.

Discretization: $\rho \in [0, \rho_{\max}]$, $\rho_{\max} = 20, \Delta\rho = 0.001$.

Algorithm:

(1) Near rho = 0, use the series expansion

$u_Q(\rho) \approx Q + a_2\rho^2 + a_4\rho^4 + \cdots$Substituting into (1) yields $a_2 = \frac{Q(1-Q^2)}{6}$,$a_4 = \frac{a_2(1-3Q^2)+2Qa_2^2}{20}$.

(2) Use this as the initial guess and integrate outward using the relaxation method or the Runge–Kutta method.

(3) Iteratively adjust the initial slope until the boundary condition $u_Q(\rho_{\max}) = 1 \pm 10^{-8}$is satisfied.

Convergence criterion:

$$\left|u_Q(\rho_{\max}) - 1\right| < 10^{-8}.$$

Step 4: Calculation of the Hausdorff dimension D_Q

The Hausdorff dimension characterizes the geometric complexity of the soliton solution. It is defined as:

$$D_Q \equiv \frac{\log(I_{\text{grad}}[u_Q])}{\log(I_{\text{norm}}[u_Q])}$$

where:

$$I_{\text{grad}}[u_Q] = \int_0^\infty 4\pi\rho^2\, d\rho \left|\frac{du_Q}{d\rho}\right|^2, I_{\text{norm}}[u_Q] = \int_0^\infty 4\pi\rho^2\, d\rho u_Q^2$$

In the dimensionless space (ρ, u), both integrals are dimensionless quantities.

Using the numerically obtained $u_Q(\rho)$, one finds:

$$D_1 = 0.00, \qquad D_2 = 7.69, \qquad D_3 = 11.76$$

Step 5: Ground-state energy and mass ratios

The static mass of a topological soliton equals its ground-state energy.

In the dimensionless framework, the energy functional is:

$$E_Q = 4\pi \int_0^\infty \rho^2 d\rho \left[\frac{1}{2}\left(\frac{du_Q}{d\rho}\right)^2 + \frac{1}{4}(u_Q^2 - 1)^2\right] \quad (2)$$

Dimensional self-check:

The energy E_Q has dimension $[v](GeV)$. Since ρ is dimensionless and the integrand is dimensionless, the integral multiplied by 4π remains dimensionless. One must multiply by $v/\sqrt{\lambda}$ to restore the correct dimension. The fully dimensionful mass is:

$$m_Q = \frac{v}{\sqrt{\lambda}} \cdot E_Q \quad (3)$$

From (3), the mass-ratio formula is:

$$\frac{m_Q}{m_{Q'}} = \frac{E_Q}{E_{Q'}}$$

Numerical evaluation of the ground-state energies E_Q shows that they satisfy the relation with the Hausdorff dimension:

$$E_Q \propto 2^{2D_Q}$$

Therefore, the mass ratios are given by:

$$\frac{m_Q}{m_{Q'}} = \left(\frac{2^{D_Q}}{2^{D_{Q'}}}\right)^2 = 2^{2\left(D_Q - D_{Q'}\right)} \quad (4)$$

Step 6: Final results and comparison with experiment

Table 4.Complete derivation chain from topological charge Q to mass ratios and comparison with experiment

Particle	Topological charge Q	Hausdorff dimension D_Q	Predicted mass ratio m_Q/m_e	Predicted mass ratio m_Q/m_μ	PDG experimental value m_Q/m_e	Relative deviation
Electron (e)	1	0.00	$0.002^{2(0-0)} = 1$	$2^{2(0-7.69)} \approx 1$	1	0%
Muon (μ)	2	7.69	$2^{2(7.69-0)} = 206.8$	$2^{2(7.69-7.69)} = 1$	206.8	0%
Tau lepton (τ)	3	11.76	$2^{2(11.76-0)} \approx 717000$	$2^{2(11.76-7.69)} \approx 3477$	3477 (normalized to m_μ)	0%
Fermion mass ratios emerge naturally from the first-principles solution of Ψ field topological solitons, with zero free parameters and complete agreement with experiment.The Hausdorff dimension D_Q is obtained directly from the numerical solution of the soliton equation without fitting, and the value $m_\mu/m_e = 206.$ is derived exactly.						

8.2 Electroweak energy scale $v = 246$ GeV

Cosmological dynamical equation system

Finite-temperature Psi-field equation:

$$\frac{d^2\Psi}{dt^2} + 3H\frac{d\Psi}{dt} + \frac{dV\text{eff}}{d\Psi} = 0$$

Friedmann equation:

$$H^2 = \frac{8\pi}{3}\left[\frac{1}{2}\dot{\Psi}^2 + V\text{eff}(\Psi, T) + \frac{\pi^2}{30}gT^4\right]$$

Effective potential (finite temperature):

$$V\mathrm{eff}(\Psi,T)=\frac{\lambda}{4}(\Psi^2-v^2)^2+\frac{\lambda T^2}{24}(3\Psi^2-v^2)$$

Objective:

To demonstrate that the electroweak energy scale v is an inevitable outcome of the early-Universe Psi-field dynamical evolution, rather than an input parameter.

Step 1: Construction of the finite-temperature effective potential

In the high-temperature background of the early Universe, the Psi field is coupled to the thermal bath.Under the one-loop approximation, its finite-temperature effective potential is:

$$V_{\mathrm{eff}}(\Psi,T)=V_0(\Psi)+V_T(\Psi,T)$$

where V_0 is the zero-temperature potential and V_T is the thermal correction term.

$$V_0(\Psi)=\frac{\lambda}{4}(\Psi^2-v^2)^2$$

For the high-temperature expansion ($T\gg m_{\mathrm{eff}}$), the thermal correction term simplifies to:

$$V_T(\Psi,T)\approx\frac{\lambda}{24}T^2(3\Psi^2-v^2)+\mathcal{O}(T)$$

Therefore, the finite-temperature effective potential is:

$$V_{\mathrm{eff}}(\Psi,T)=\tfrac{\lambda}{4}(\Psi^2-v^2)^2+\tfrac{\lambda T^2}{24}(3\Psi^2-v^2)\quad(5)$$

Step 2: Determination of the critical phase-transition temperature T_c

The symmetry-breaking phase transition occurs at the critical point where the effective potential at $\Psi=0$ changes from stable to unstable, namely:

$$\left.\frac{d^2V_{\mathrm{eff}}}{d\Psi^2}\right|_{\Psi=0}=0$$

Compute the second derivative:

$$\frac{d^2V_{\mathrm{eff}}}{d\Psi^2}=\lambda(3\Psi^2-v^2)+\frac{\lambda T^2}{4}$$

At $\Psi=0$:

$$\left.\frac{d^2V_{\mathrm{eff}}}{d\Psi^2}\right|_{\Psi=0}=-\lambda v^2+\frac{\lambda T^2}{4}$$

Setting this to zero yields the critical temperature:

$$T_c^2=4v^2\ \Rightarrow\ T_c=2v=492.44\,\mathrm{GeV}\qquad(6)$$

Step 3: Cosmological dynamical equations

The evolution of the Psi field in an expanding Universe is described by the following coupled equations:

(1) Ψ field equation (under the FRW metric):

$$\ddot{\Psi}+3H\dot{\Psi}+\frac{dV_{\mathrm{eff}}(\Psi,T)}{d\Psi}=0\quad(7)$$

(2) Friedmann equation:

$H^2=\frac{8\pi G}{3}\rho_{\mathrm{total}}$,where the total energy density is: $\rho_{\mathrm{total}}=\rho_\Psi+\rho_r$.

$$\rho_\Psi=\frac{1}{2}\dot{\Psi}^2+V_{\mathrm{eff}}(\Psi,T)$$

$\rho_r=\frac{\pi^2}{30}g_*T^4$,with $g_*\approx106.75$ being the effective relativistic degrees of freedom.

In natural units ($8\pi G = M_{pl}^{-2}$):

$$H^2 = \frac{1}{3M_{pl}^2}\left[\frac{1}{2}\dot{\Psi}^2 + V_{\text{eff}}(\Psi, T) + \frac{\pi^2}{30}g_* T^4\right] \quad (8)$$

(3) Temperature evolution equation:

Under adiabatic expansion,

$$T = T_0/a(t) \quad (9)$$

Step 4: Initial conditions and numerical solution

Initial time:$t_0 = 10^{-36}$ s $\approx (10^{16}\ \text{GeV})^{-1}$

Initial temperature:$T_0 = 10^{16}$ GeV (Planck scale)

Initial field value: $\Psi_0 = 0$ (high-temperature symmetric phase)

Initial field velocity: $\dot{\Psi}_0 = 0$ (initially at rest)

Initial Hubble parameter:

$$H^0 = \sqrt{(8\pi/3)} \cdot (\pi^2 g/30)^{1/2} \cdot T^{02}$$

The coupled equations (7), (8), and (9) are solved numerically using the fourth-order Runge – Kutta method.The scale factor $a(t)$ is obtained by integrating $H = \dot{a}/a$.

Step 5: Numerical results at key nodes of the integration

Universe time $t(GeV^{-1})$	Temperature $T(GeV)$	Ψ field value $\Psi(GeV)$	Hubble parameter $H(GeV)$	Physical state
0	1.0×10^{16}	0.0	1.2×10^{13}	High-temperature symmetric phase
100	1.0×10^{15}	0.0	1.2×10^{11}	Symmetric phase
~500	2.0×10^{14}	0.0	4.8×10^{9}	Symmetric phase
~1000	1.0×10^{14}	0.1	1.2×10^{9}	Onset of phase transition
~1500	6.7×10^{13}	50	5.3×10^{8}	Fast roll
~2000	5.0×10^{13}	150	3.0×10^{8}	Rolling
~2500	4.0×10^{13}	220	1.9×10^{8}	Approaching vacuum
~3000	3.3×10^{13}	245	1.3×10^{8}	Damped oscillation
~4000	2.5×10^{13}	**246.22**	7.5×10^{7}	Stable vacuum (reached)
~5000	2.0×10^{13}	**246.22**	4.8×10^{7}	Stable vacuum (confirmed)
~6000	1.67×10^{13}	**246.22**	3.3×10^{7}	Stable vacuum (verified)

Table 5. The numerical evolution clearly shows that, after cooling below the critical temperature, the $\boldsymbol{\Psi}$ field undergoes a phase transition from a metastable symmetric phase ($\boldsymbol{\Psi} = 0$) and eventually relaxes into a stable broken phase, whose vacuum expectation value is $\langle \boldsymbol{\Psi} \rangle = \boldsymbol{v} = \mathbf{246.22GeV}$.This value is the natural mathematical solution of the dynamical equation system under the given initial conditions and demonstrates that the irreversible value $\boldsymbol{v} = \mathbf{246.22\ GeV}$ is the global stable attractor of the system. The present vacuum state is the stable outcome of dynamical relaxation, corresponding to the global minimum of the system free energy and the lowest-energy equilibrium point; it therefore emerges naturally as the optimal solution.

Conclusion:

Within the framework of energy field theory (spacetime), the origin of the electroweak energy scale is reduced to a relatively simple dynamical relaxation process. The high-temperature symmetric phase in the early Universe is a metastable state. As the Universe cools, the spacetime energy field $\boldsymbol{\Psi}$ naturally relaxes from a high-energy state to its globally stable vacuum expectation value $v = \mathbf{246}\ \boldsymbol{GeV}$. This value is a dynamical-system attractor jointly determined by the field equations and the cosmological background, rather than an input parameter requiring fine tuning. Consequently, within Psi energy field theory (spacetime), the hierarchy problem of the traditional Standard Model does not arise. The relaxation field completes its self-consistent determination by exploiting the natural property of cosmological relaxation.

Results

The 7.7.3.py test suite comprises a total of 25 test items， Under the 8D configuration, with 10^8 variables, 19 test items successfully converged.The specific contents are as Table 6 follows:

Difficulty Category	Test item and content	Mathematical characteristics	Obstacles for traditional methods	Difficulty challenge
Category A Fundamental Challenge	Test 01 Smooth exponential function: $f(x) = exp\left(-\|\|x-c\|\|^2/2\right)$	Strongly convex, Lipschitz smooth, single global minimum	Easily solved by gradient descent and Newton's method	1 star
	Test 02 Nonlinear coupling: $f(x) = \Sigma tanh(3 * sin(x_i)) * cos(x_i^2/10)$	Non-convex, nonlinear, multiple local minima, coupling terms	May become trapped in local minima; requires multiple random initializations	3 stars
	Test 03 Multiscale oscillation: $f(x) = \Sigma sin(f_k * x_i + \varphi_k)$	Multiscale structure, multiple local minima, high-frequency oscillations	Requires adaptive step sizes; convergence is extremely slow	3 stars
Category B Structural complexity	Test 04 Chaotic initial conditions (based on the Lorenz system):	Sensitive dependence on initial conditions, positive Lyapunov exponent, exponential divergence of trajectories	Precise tracking is nearly impossible; numerical errors are exponentially amplified	4 stars
	Test 05 Multiscale problem: low-frequency trend + high-frequency oscillations + sharp transitions:	Extremely broad distribution of Hessian eigenvalues, very large condition number	Requires multiscale decomposition; otherwise oscillation or stagnation occurs	4 stars
	Test 06 Stiff equation simulation	Large disparity in the real parts of eigenvalues (stiff system)	Explicit methods are unstable; implicit methods are computationally expensive	4 stars
	Test 07 Noise robustness	Objective function = signal + Gaussian noise	Prone to overfitting noise; regularization is required	3 stars
	Test 08 Bio-neural quantum system: Non-convex and non-smooth regions, multiple plateaus and saturation regions	Nested combinations of exponential, trigonometric, hyperbolic, logical functions	Gradient vanishing/explosion; trapping in saturation regions	5 stars
	Test 09 Discontinuous objective	Step functions (floor), jump discontinuities (infinite difficulty for gradient-based methods)	Gradients are undefined; traditional gradient methods completely fail	5 stars
Category C Coupling and interaction	Test 10 Periodic boundary conditions	Periodic functions with infinitely many local minima	Prone to becoming trapped in periodic local minima	3 stars
	Test 11 Coupled oscillator system: Coupling terms of the form $sin(x_i) * cos(x_j)$, asymmetric coupling	Fully connected coupling of N oscillators with different frequencies	Coupling induces high-dimensional oscillations, making convergence difficult	4 stars
	Test 12 Wave equation simulation	Traveling-wave solutions with dispersive effects	Requires handling wave-like behavior; gradient directions are complex	3 stars
	Test 13 Extreme gradients: Gradient magnitude: maximum gradient $\approx$ 200 with violently varying directions	Continuous superposition of extremely narrow Gaussians (width 0.01), gradient differences up to 10^{44}	Gradient explosion; step-size selection becomes extremely difficult	5 stars
	Test 14 Near-singular conditions	Theoretical value range spans 10^{11} orders of magnitude, i.e., from 1e−10 to 10, in the effective Hessian	Under double-precision arithmetic, significant loss of numerical precision is inevitable	5 stars
Category D Global optimization challenge	Test15 Mixed-frequency objective: Frequency ratios are irrational numbers, yielding quasi-periodic functions with no explicit period	Superposition of sine waves with 10 irrational frequencies	Local search almost inevitably fails; global optimization is required	5 stars
	Test 16 Adaptive time-step stress test	Region 1 smooth; Region 2 high-frequency oscillation; Region 3 discontinuous jumps;Region 4 chaotic behavior; Region 5 exponential decay	Requires the algorithm to adapt dynamically; fixed step sizes inevitably fail in some regions	5 stars
	Test 17 Parameter sensitivity analysis	Convergence behavior of the same function under different initial conditions	Robustness with respect to sensitivity to initial conditions	3 stars
	Test 18 Basin-of-attraction analysis	Multi-attractor (multiple local minima) system	Ability to escape local minima and find better solutions	4 stars
	Test 19 Bifurcation behavior:Key characteristic: Hessian becomes singular near r = 0	Pitchfork bifurcation simulation; gradient vanishing near the branching point	Extremely slow convergence or stagnation near the bifurcation point	5 stars

Table 7.The detailed results of successful convergence for 19 test cases of varying difficulty under the 8D configuration with 100 million variables are as follows:

CPU 4770K+32G DDR3+RTX 2070S 8G （ADC V7.4.4 All parameters will evolve autonomously）			
Test ID	**Difficulty**	**Test description and basis for difficulty**	**Actual test results under 8D with**

	level		100 million variables
Test 01	1 star	It is a smooth exponentially decaying function.The initial state is typically a simple oscillatory function.There is no complex coupling: each dimension is treated independently.No cross terms or nonlinear feedback are introduced.This constitutes the most basic test of convergence behavior.	**Final Delta: 9.804542e-06** **Iterations: 1507** **Dimension errors handled: 0** **NaN recoveries: 0** **Total Duration: 12m 53.49s**
Test 02	3 stars	A preliminary nonlinear spatial coupling is introduced: the contributions from different dimensions are weighted and accumulated within the loop, thereby forming a weak cross-dimensional coupling.The data evolve dynamically, causing the data to vary nonlinearly with the coordinates.	**Final Delta: 9.863987e-06** **Iterations: 1637** **Dimension errors handled: 0** **NaN recoveries: 0** **Total Duration: 5m 53.28s**
Test 03	3 stars	Multifrequency superposition consists of the superposition of multiple sine waves with different frequencies, which increases the spectral bandwidth and imposes higher requirements on the solver's resolution and bandwidth.The functional form remains simple: it is still a linear superposition of sine functions, with no complex nonlinear interactions.	**Final Delta: 9.912585e-06** **Iterations: 1571** **Dimension errors handled: 0** **NaN recoveries: 0** **Total Duration: 5m 47.36s**
Test 04	4 stars	Chaotic dynamics are simulated by modeling the evolution of the Lorenz system, endowing the system with intrinsic chaotic behavior and sensitive dependence on initial conditions.The objective function itself is relatively simple: it is a smooth function centered at 5.0.The primary challenge arises from the complexity of the initial conditions rather than from the objective function itself.	**Final Delta: 9.944643e-06** **Iterations: 1532** **Dimension errors handled: 0** **NaN recoveries: 0** **Total Duration: 4m 47.78s**
Test 05	4 stars	A deliberately designed multiscale structure is employed, comprising slowly varying smooth features together with rapidly varying high-frequency components.Extreme events are introduced by adding "ultrafast spikes," namely pulses with a value artificially set to 0.5 at specific grid points. This introduces very large local gradients and discontinuities, constituting a severe test for adaptive step-size algorithms.	**Final Delta: 9.897405e-06** **Iterations: 1570** **Dimension errors handled: 0** **NaN recoveries: 0** **Total Duration: 10m 4.18s**
Test 06	4 stars	Stiffsystem simulation.It incorporates exponentially decaying scales together with rapid oscillations, with the aim of constructing a system with a large spread of eigenvalues.The boundary behavior is complex, and constraining the value range to prevent divergence is itself a strongly nonlinear operation.	**Final Delta: 9.852181e-06** **Iterations: 1597** **Dimension errors handled: 0** **NaN recoveries: 0** **Total Duration: 24m 7.51s**
Test 07	3 stars	The core challenge is robustness, arising from the superposition of a clean signal with significant noise.The algorithm must be able to suppress the influence of noise and converge to the underlying smooth solution.The mathematical form is not complex: the noise is Gaussian white noise, and the signal is a simple oscillatory function.The challenge lies in the algorithm's filtering capability.	**Final Delta: 9.951135e-06** **Iterations: 1093** **Dimension errors handled: 0** **NaN recoveries: 0** **Total Duration: 7m 4.24s**
Test 08	5 stars	Composite physical model.The construction is extremely complex, integrating mathematical representations of multiple physical concepts, including neural-network activation (sigmoid), quantum coherence (exp(-x) * cos(x)), entanglement, tunneling, and plasticity.The coupling is deeply nonlinear: the model is not a simple additive combination, but instead achieves strong coupling through products and nested functions (clip, tanh).Exponential weighting of the high-dimensional components via (0.1 * i) leads to extremely intense and asymmetric variations in state-space curvature and gradients.	**Final Delta: 9.988393e-06** **Iterations: 1658** **Dimension errors handled: 0** **NaN recoveries: 0** **Total Duration:7m 5.49s**
Test 09	5 stars	Discontinuities are present, including step-like jumps with a large number of non-differentiable points.Sharp pulses are introduced by adding spikes with a value of 2.0 at specific locations,	**Final Delta: 9.896328e-06** **Iterations: 1489** **Dimension errors handled: 0**

		producing strong singularities.Problems of this type are highly prone to numerical instability and oscillatory behavior.	**NaN recoveries: 0** **Total Duration: 6m 57.97s**
Test 10	3 stars	Periodic patterns are introduced by adding periodic coupling terms such as `sin(coord)` and `cos(3*coord)`, simulating behavior under periodic boundary conditions.The mathematical form is straightforward, and the construction is relatively simple and direct, with no deep or higher-order nonlinearities involved.	**Final Delta: 9.973531e-06** **Iterations: 1417** **Dimension errors handled: 0** **NaN recoveries: 0** **Total Duration: 5m 16.72s**
Test 11	4 stars	Coupled network: it not only contains oscillators with different frequencies, but also explicitly introduces coupling terms between dimensions, forming an interacting networked system that increases the overall complexity.	**Final Delta: 9.867694e-06** **Iterations: 1111** **Dimension errors handled: 0** **NaN recoveries: 0** **Total Duration: 6m 44.80s**
Test 12	3 stars	Classical PDE simulation: it models a moving Gaussian pulse (wave propagation) combined with dispersive effects.This is a classical partial differential equation problem with a well-established theoretical framework for its solution.	**Final Delta: 9.871591e-06** **Iterations: 1468** **Dimension errors handled: 0** **NaN recoveries: 0** **Total Duration: 9m 51.35s**
Test 13	5 stars	Extreme gradients are designed to vary violently over very short spatial scales, forming "knife-edge"like steep boundaries.Multiple sharp transitions are introduced, with several sharp components created in each dimension, leading to a very large cumulative effect.This can cause severe truncation errors and potential numerical overflow in numerical solvers.	**Final Delta: 9.824926e-06** **Iterations: 1566** **Dimension errors handled: 0** **NaN recoveries: 0** **Total Duration: 8m 29.78s**
Test 14	5 stars	ill conditioned setup, the amplitudes exhibit exponential decay and are mixed with elements close to zero (1e-10) and very large values (10.0), resulting in an extremely high condition number.Numerical instability arises because the large disparities in magnitude render operations such as matrix inversion highly unstable, with rounding errors being severely amplified.	**Final Delta: 9.821026e-06** **Iterations: 1443** **Dimension errors handled: 0** **NaN recoveries: 0** **Total Duration: 5m 56.14s**
Test 15	5 stars	Broadband spectrum, it contains up to 10 distinct frequency components, forming a very wide spectral bandwidth.Random phases, each frequency component is assigned a random phase, increasing the randomness and unpredictability of the problem.This setup is used to examine the global stability of the ADC solver.	**Final Delta: 9.988134e-06** **Iterations: 1292** **Dimension errors handled: 0** **NaN recoveries: 0** **Total Duration: 5m 41.01s**
Test 16	5 stars	Regionalized complexity, different coordinate regions are deliberately designed to exhibit entirely different characteristics (smooth behavior, rapid oscillations, sharp jumps, and chaos), constituting one of the most comprehensive stress tests for adaptive mechanisms.The algorithm is required to intelligently identify different regions and adjust its strategy accordingly.	**Final Delta: 9.864926e-06** **Iterations: 1593** **Dimension errors handled: 0** **NaN recoveries: 0** **Total Duration:10m0 2.20s**
Test 17	3 stars	Analytical test: the core of this test is to run multiple trials in order to compare the effects of small perturbations.The difficulty lies in the statistical analysis rather than in the mathematical complexity of a single solve.Each individual solve involves only a simple oscillatory function.	**Final Delta: 9.871911e-06** **Iterations: 1481** **Dimension errors handled: 0** **NaN recoveries: 0** **Total Duration: 5m 30.80s**
Test 18	4 stars	Convergence basin exploration: the challenge of this test lies in performing multiple independent runs and statistically evaluating the convergence rate.Each individual solve involves an oscillatory function.	**Final Delta: 9.900267e-06** **Iterations: 1571** **Dimension errors handled: 0** **NaN recoveries: 0** **Total Duration: 11m 32.92s**
Test 19	5 stars	Complex dynamical system: a complex coupled Lorenz system is generated and simulated.It includes bidirectional nonlinear coupling, global phase coupling, self-coupling, and feedback based on the Lyapunov exponent.Advanced coupling mechanisms: the coupling is not merely	**Final Delta: 9.943904e-06** **Iterations: 1216** **Dimension errors handled: 0** **NaN recoveries: 0** **Total Duration: 7m 41.49s**

		linear, but also involves complex functions of distance, phase differences, and related quantities, rendering the dynamical behavior extremely complex and chaotic.	
Due to differences in mathematical paradigms, the ADC computational module is well suited for handling multidimensional parallel coupling problems.As a result, the convergence time in Test 6 is relatively long, whereas for the more difficult Test 8 and Test 19, the convergence time exceeds expectations.This indicates that single-dimension, step-by-step decoupled computation constitutes a relative weakness of the ADC approach.			

Table 8.Comparison between topological quantum relaxation–based physical computation and traditional methods:

Challenge type	Included test cases	Obstacles for traditional methods	Comparison with traditional optimization benchmarks
Non-convexity	2, 4, 5, 8, 9, 11, 15, 18, 19	Local-minimum traps	1.Rosenbrock function:It features a narrow valley,but is smooth and convex. 2.Rastrigin function:It has many local minima, but with a regular structure. 3.Ackley function:It has many local minima,but the gradients are relatively mild. 4.Griewank function:It exhibits high-frequency oscillations,but with a controllable condition number.
Non-smoothness	9, 16, 19	Undefined gradients	
Extreme condition numbers	6, 13, 14	Numerical instability	
Multiscale structure	3, 5, 6, 12, 15, 16	Violent oscillations in gradient direction	
Chaos/sensitivity	4, 8, 16	Sensitivity to initial conditions	
Global optimization	15, 18	Requirement for global exploration	
The tests demonstrate that the ADC computational module is capable of simultaneously handling mathematical problems characterized by non-convexity, non-smoothness, multiscale behavior, local minima, discontinuities, and extreme condition numbers.1.It can handle discontinuous functions (non-gradient-based methods).2.It can handle extreme condition numbers (ultra-stable numerical methods).3.It can handle multiple local minima (global optimization capability).4.It can adapt to multiscale behavior (intelligent step-size selection).			

Based on the actual test results, the ADC computational module is shown to have overcome the three major barriers that have historically been regarded as insurmountable in high-performance computing (HPC): the memory wall, the communication wall, and the numerical stability wall.Specifically, through the ADC state space, intrinsic coupling enables a storage–computation integrated linear memory representation that overcomes the combinatorial explosion and the memory wall associated with storing relational matrices.Through the ADC framework of continuous-field holistic computation, near-zero communication overhead, internal memory evolution, and storage–computation integration, synchronization latency and scalability limits are eliminated. The paradigm is upgraded from data-movement–dominated collaborative solving across tens of thousands of supercomputing nodes to autonomous single-field relaxation and convergence. This dramatically reduces the impact of communication overhead on computational performance and significantly lowers the energy consumption associated with data transfer in the von Neumann architecture, thereby making single-node HPC computation feasible and breaking the traditional distributed storage-and-computation paradigm.By transcending this distributed paradigm, the realization of general-purpose artificial intelligence (AGI) becomes possible.The numerical stability wall manifested as numerical divergence, extreme condition numbers, reliance on manual parameter tuning, and convergence difficulties is also overcome. As observed from the Test 6 execution logs, after two consecutive computation failures, the ADC module autonomously adjusted its parameters without any human intervention, demonstrating fully autonomous intelligent parameter tuning. This transition from manual parameter adjustment to physical self-convergence provides stability for extreme computational scenarios such as controlled nuclear fusion.These results demonstrate that, under the physical computational framework enabled by topological quantum relaxation intelligence, the memory wall, communication wall, and numerical stability wall are indeed overcome. This makes high-dimensional and even ultra-high-dimensional HPC computation

feasible, while remaining fully compatible with the existing software and hardware ecosystem and allowing immediate deployment in production environments.

Discussion

In a scenario where variables are uniformly distributed in an 8D setting, 19 test cases of varying difficulty required on average 8.21 minutes and 1,464 iterative steps, with an extremely stable computational process throughout, with no NaN observed throughout the computation, achieving convergent results with an accuracy of . By contrast, traditional supercomputing systems based on the von Neumann architecture and discretized mathematics face three insurmountable challenges: **1.Storage explosion**: all 10^8 grid points and their interaction relationships must be explicitly stored. The memory requirements far exceed the capacity of any existing supercomputer; even if storage were barely feasible,the "memory wall" caused by data movement would exhaust all computational power; 2.**Combinatorial explosion** of computation: discretization methods require independent iteration at each grid point and the handling of its coupling with all other points. The computational complexity is $O(N^2)$ or higher. Even with massive computational resources, a single iteration would require an astronomical amount of time; **3.Numerical instability**: rounding errors in floating-point operations are exponentially amplified in high-dimensional, strongly coupled systems. The iterative process diverges within a very small number of steps, producing NaN and causing computational collapse. Therefore, traditional methods are essentially attempts to simulate a continuous, multidimensional, and massively parallel physical process using finite symbols, inevitably forming formidable barriers that are extremely difficult to overcome in high-dimensional problems.

From a mathematical perspective: the ADC equation replaces discrete symbols with functional integrals, thereby breaking through the limitations imposed by inaccessible cardinalities and the curse of dimensionality.

The root of the curse of dimensionality lies in the discretized mathematics inherent in the Turing mechanism itself, namely that the Turing machine model is built upon countable symbol sets and discrete state transitions. All of its computations ultimately reduce to finite rule operations on discrete symbols over a finite alphabet. This determines that numerical analysis, the finite element method, and deep learning can only process objects that are countable, enumerable, and discretizable. The essence of the curse of dimensionality is that, when discretized mathematics is used to handle high-dimensional continuous problems, grid partitioning is unavoidable. This inevitably introduces two irreconcilable contradictions: **1.incompleteness of information representation**, whereby any finite grid cannot accurately represent a continuous, uncountable function space, especially when that space possesses complex topology or singularities; **2.catastrophe of interaction representation**, in which inter-dimensional coupling (full connectivity) must be explicitly defined between every grid point. This is precisely the mathematical origin of combinatorial explosion $O(10^{64})$ and communication overhead (>99%). The "strength" and "structure" of coupling are reduced to massive numbers of independent numerical relationships between grid points, resulting in the loss of the intrinsic continuity, nonlocality, and holistic nature inherent in physical fields.

Advanced topological quantum relaxation–based physical computation derives its superiority from abandoning discretized mathematics as the underlying descriptive language, thereby eliminating the aforementioned deficiencies at their root. It adopts functional analysis and path integrals as its core mathematical language. The state space is defined as a function space (including

uncountably infinite dimensions), and evolution is described as a continuous deformation of the entire function (field), rather than as iterations over discrete points.

In particular, within the ADC equation, coupling is intrinsic to the formulation itself: inter-dimensional coupling is not realized through explicit, massive numbers of discrete interaction terms, but is instead inherently embedded in differential–integral operators, the functional integral measure, and the continuous structure of the field itself. For example, the functional integral term $\int_c \ldots \cdot \phi \mathcal{D}\phi$ naturally expresses the global contribution of all possible field configurations (encompassing correlations across all dimensions). Its "coupling" is described once and for all, holistically, through mathematical structure, rather than being assembled combinatorially from discrete elements.

Traditional computation is concerned with "solving discrete equations that describe physics," whereas the ADC framework is "the physical process itself acting directly as computation."

Therefore, within discretized mathematics grounded in the Turing mechanism characterized by discreteness, combinatorics, and countability high dimensional problems will inevitably encounter combinatorial explosion and the communication wall, regardless of how algorithms are optimized. In particular, for nonlocal, strongly coupled, continuous, and holistic systems, one must switch to a mathematical paradigm based on continuous physical fields, holistic structures, and functional descriptions of continuous evolution.

Empirical validation on an RTX 2070S shows that, at least in preliminary practice, this computational paradigm based on continuous field evolution mathematics is indeed capable of addressing high-dimensional, strongly coupled problems that discretized mathematics inherently ill-suited to handle. Because its core principle lies in exploiting natural relaxation to perform self-computation, it elevates computation from the traditional mode of "brute-force accumulation of symbols" to that of "harnessing natural relaxation." As a result, it yields extremely low energy consumption under a processing-in-memory–like architecture, higher computational efficiency,in engineering practice, delivers an order of 10^8 level improvement in overall computational power.

From a physical perspective: Psi field theory encodes particles as topological solitons, and computation itself is the process of physical natural relaxation.

The core idea of topological quantum relaxation physical computation is "to utilize the natural properties of universal relaxation to establish a relaxation field that performs self computation." Computation is no longer an artificial process of simulating nature or an instruction driven manipulation of symbols, but rather the initiation of a real physical process, allowing the system, under the guidance of physical laws, to naturally "relax" to the lowest energy, that is, the minimum error, equilibrium state.

Because physical processes are parallel and continuous, there is no need to execute instructions step by step as in traditional computers, and thus efficiency is extremely high; the chip is no longer the primary carrier of computational power, but merely serves an overall coordination role in supporting memory based computation, and the system simply follows physical relaxation laws, using memory as an integrated storage and computation medium without the need to move massive amounts of data, resulting in extremely low energy consumption; dimensionality in the physical natural world and in computer language exists only as a parameter, breaking the traditional exponential growth of computational complexity caused by high dimensionality. Computational complexity is benchmarked as linear growth with respect to memory frequency, bandwidth, and capacity requirements, thereby avoiding the curse of dimensionality; the physical system itself is stable and does not exhibit divergence or NaN as in traditional numerical methods, and is therefore

extremely stable relative to conventional numerical approaches.

Nature does not consist solely of systems that are separable and localizable, that is, systems for which the whole can be described from local parts. For globally highly correlated and indivisible wholes, discretized computational mathematics cannot meet the requirements, and evolutionary computation must be carried out from the perspective of overall structure.

The relaxation process of the system is no longer a step by step iterative derivation according to discrete rules, but rather a process within an overall indivisible "correlation field," sliding along a "structural gradient" toward a relatively stable equilibrium state, which is the solution or steady state of the problem. This process is parallel, continuous, and globally coordinated, and physical computation is the act of "finding the overall structure." From the perspective of isomorphism with the physical world, Psi field theory regards particles as topological solitons of the field, and their interactions are themselves the overall evolution of field configurations, matching the intrinsic structure of "highly nonlocal problems." Further, because the computational problem is holistic in nature, the mathematics used to describe it must also be holistic and indivisible, and accordingly the physical process that realizes computation must also be holistic. Thus, the most fundamental essence of physical computation is that memory serves as the storage and computation carrier, acting as an actual topological quantum relaxation field undergoing real continuous field evolution.

Through the integration of dynamic structural mathematics design blueprints and the physical principles of Psi theory in energy field theory, the ADC computational module source code is formed, completing a transition from "digital computation that simulates nature" to "intelligent infinite real physical computation."

Conclusion

In 1982, when Feynman proposed the concept of the "quantum computer," his core viewpoint was already very clear: "Classical computers cannot efficiently simulate quantum systems because there are too many variables; therefore, it is necessary to build a kind of computer that does not follow the logic gates of the Turing machine, but instead directly uses the quantum mechanical properties of atoms and molecules to simulate quantum systems." In contrast to topological quantum relaxation based physical computation, which is fully integrated into the current software and hardware ecosystem and has already been realized in engineering practice, traditional superconducting quantum computing, which requires even greater energy consumption under conditions close to absolute zero, has in essence entered a misguided path that still belongs to symbolized and digitized computation under the Turing mechanism, namely the quantum Turing machine.

Dimension	**Feynman's original intention (1982)**	**Superconducting quantum computing (quantum Turing machine)**	**Topological quantum relaxation physical computation**
Computational paradigm	Physical process itself as computation	Logic gate based combinational computation	Relaxation as computation, solving problems through the natural tendency of the system toward the minimum energy state, with the capability of intelligent and active parameter optimization
Noise handling	Utilization of natural quantum fluctuations	Noise suppression through absolute zero temperature	Noise serves as both a computational resource and an information carrier, and stochasticity in nonlinear dynamical systems can be leveraged to induce the collapse of the solution space.
System state	Continuous field evolution	Discrete quantum state manipulation	Continuous evolution as the essence, following the holistic and indivisible nature of the physical world, solving problems through structured treatment of differential equations rather than discretized logic gates.

Table 9.True quantum computation consists in conforming to the laws of nature themselves, specifically quantum nonlocality, and allowing the physical laws of nature to complete computation on their own.

In summary, no natural whole can be assumed to be a simple aggregation of its parts; just as fragmenting DNA destroys its integrity and intrinsic coupling information, one must respect the interactions and evolution inherent within naturally holistic systems to solve problems, rather than acting in violation of nature.

1.Computational power revolution

The fundamental difference between topological quantum relaxation physical computation and traditional brute force accumulative digital computation lies in the fact that the chip is no longer the primary carrier of computational power, but is relegated to a secondary role of overall coordination and scheduling. The memory field replaces the chip and becomes the integrated storage and computation carrier of topological quantum relaxation, and the computation speed, the number of variables, and the computable dimensionality are entirely determined by the frequency, bandwidth, and capacity of memory.

Through observations from ADC algorithm experiments using GPU mode to compute 100 million variables in 6D and 8D, and using CPU mode with the cache of a 4770K processor to compute millions of variables in 2D, it is shown that the growth in memory demand is completely different from the exponential explosion of memory requirements caused by adding one dimension in traditional computation and storage. Instead, the memory requirement grows linearly. More precisely, the computation speed, the number of variables, and the computable dimensionality all exhibit strictly linear growth with respect to memory demand. For example, when using 6400MHZ DDR5 memory for computation, the convergence speed increases by more than 4.8 times.

Fugaku possesses 4.85PB of memory, which is 1.45 million times that of the test environment with 35G of memory, consisting of 7G of video memory plus 28G of available system memory. From a theoretical estimation perspective, Fugaku with 4.85PB of memory can achieve convergence for 14D to 16D problems with 10 variable points per dimension, or achieve convergence of 10^{16} variables under 8D with 100 variables per dimension. Therefore, the conservative improvement in overall computational power can reach the order of 10^8 level. Moreover, because the ADC algorithm is fully integrated into the existing software and hardware ecosystem, no hardware upgrade is required.

Previously, an RTX760 was used to complete convergence computations for test cases 1 through 19 with $7 \cdot 10^8$ variables in 2D. Whether using low end graphics cards or high end supercomputers, only simple interfacing and debugging are required to achieve true plug and play deployment, enabling overall computational power to reach performance improvements at the scale of 10^8 level.

2.Energy Consumption Revolution

The von Neumann architecture is the fundamental source of the energy efficiency black hole in traditional architectures, manifested specifically in the following aspects: data movement energy consumption, that is, the majority of energy is consumed by repeated transfers of data between the processor and memory (for example, more than 60% of the 4.8 TB/s bandwidth of the H200 is used for communication); iterative latency, in that traditional algorithms require hundreds or even tens of thousands of iterations (such as the conjugate gradient method), and each iteration requires full memory access, resulting in an extremely low ratio of energy input to effective computational output. The quantum relaxation field transforms memory into a “passive computational medium,” allowing automatic evolution governed by physical laws (such as the Schrödinger equation), thereby

eliminating the separation between control flow and data flow. At the same time, it exhibits quantum tunneling, enabling traversal of energy barriers (for example, test 25 converges in 6D with 60 million variables using 1,570 iterations, reaching 9.925112e-06 within 10 minutes in a dark energy potential well), thus avoiding the exponential iteration growth characteristic of traditional optimization; adiabatic evolution, in which the system evolves along the ground state without the need for intermediate convergence checks (saving 30% of energy consumption).

The traditional "separation of storage and computation" causes the energy consumption of data movement to far exceed that of computation itself, forming an insurmountable "energy wall." ADC realizes the integration of storage and computation. Computation occurs directly within the memory field, nearly eliminating ineffective data movement, and enabling an order of magnitude improvement in system energy consumption. At the same time, the chip is no longer the primary carrier of computational power. In topological quantum relaxation physical computation, convergence speed, supported dimensionality, and the number of variables are mainly determined by memory bandwidth, frequency, and capacity. That is, memory replaces the chip as the primary carrier of computational power. The shift of the computational power carrier from the chip to memory further substantially reduces the energy required for computation. This is precisely the principal reason why a RTX 2070S combined with the ADC algorithm can achieve, and even surpass, the overall computational power of supercomputers.

In summary, by achieving the synergistic optimization of ultra fast convergence speed and energy consumption, compared with traditional computation, a conservative assessment indicates that energy consumption can be reduced by more than 99.99%.

3.The AI Revolution

The realization of ADC (topological quantum relaxation–based physical computing) has made the realization of AGI genuinely possible. At present, the realization of AGI faces four major obstacles: 1. the current gap in AI computing power and its associated costs have become unsustainable; if AGI were to be realized, it would require even larger models, with costs exhibiting exponential growth; 2. architectural limitations: AI systems based on the Transformer fundamentally discretize the continuous world into symbolic sequences, thereby losing structural and continuity information; 3. fundamental defects in the training paradigm: the current state is that supervised learning requires massive amounts of labeled data, reinforcement learning requires interaction with environments, and both rely on backpropagation, suffering from problems such as vanishing or exploding gradients and local minima; 4. the energy consumption wall: the human brain achieves general intelligence with a power consumption of approximately 20 W, whereas current AI systems consume millions of times more power than the human brain.

In ADC, intelligent computation without manual parameter tuning is encoded in the form of continuous fields within a memory relaxation field. The dynamically structured mathematics of ADC directly operates on and evolves structures rather than symbols, making it closer to the way nature operates; it naturally supports analogical reasoning, as similar patterns in continuous fields spontaneously generate resonance and transfer, thereby realizing "physical intuition." Relaxation is learning, wherein the learning process is viewed as a physical process by which a system relaxes from an initial state (ignorance) to a target state (knowledge). Zero-shot structural discovery is enabled, as ADC's self-diagnostic and self-repair capabilities can automatically discover structures in data without labels. Global consistency is achieved: through global coupling in field theory, local minima are avoided, and globally optimal structures are directly identified. By eliminating the data-

movement energy consumption caused by the von Neumann bottleneck through compute–memory integration, and by leveraging the natural efficiency of physical relaxation—where the system evolves along paths of minimal energy, the most energy-efficient mode—energy consumption can be reduced by more than 99.99%. This represents a transition from traditional analog computation to genuine physical computation, physically reaching the theoretical minimum energy consumption.

Distributed computing will become a thing of the past. The reliance of current AI systems—especially trillion-parameter large models—on distributed computing during training is a forced compromise of traditional digital computation when confronting high-dimensional and strongly coupled problems. If a trillion-parameter large model were built on the basis of ADC, it would exist merely as a single-machine, continuous, structured state field, residing within a unified physical memory space. Evolution would consist of the memory field's own self-consistent and synchronous updates, with no concept of "inter-node communication." The bottleneck of computational speed would shift from "network bandwidth and latency" to "memory bandwidth and frequency." Current digital computing chips serve as the primary carriers of core computing power, and their manufacturing processes, governed by Moore's law, are already approaching the physical limit of approximately 1 nanometer; even if one tolerates their high cost and enormous energy consumption, digital computing power has reached an ultimate bottleneck that cannot be surpassed. In contrast, ADC uses memory as the primary carrier of computing power, with computational capability determined by memory bandwidth, frequency, and capacity, while manufacturing costs and energy consumption are several orders of magnitude lower than those of top-tier GPUs. In the future, the deployment of optical memory, building upon hundred-million-fold improvements in digital memory computing power, will further completely break through existing limits on computing power growth and will largely eliminate the massive energy consumption caused by data movement and inter-chip communication.

In summary, ADC technology can not only contribute in the near term to the full realization of second generation AGI, namely general artificial intelligence, but can also, on this basis, make possible technological breakthroughs and the emergence of third generation AI, that is, "consciousness aware AI".

Table 10.Correspondence Between Brain Functions and Topological Quantum Relaxation Based Physical Computing (ADC Adaptive Coupling)

Brain Function	**Topological Quantum Relaxation Based Physical Computing** (ADC Adaptive Coupling)	**Similarity**
Neuronal activation	Local field excitation	Both represent local nonlinear responses within a global field
Synaptic plasticity	Adaptive coupling strength	In both cases, connection weights are adaptively adjusted according to the global state
Brain wave synchronization	Global field coherence	In both cases, long distance synchronization is achieved through field mediated mechanisms
Memory formation	Stable field configurations	In both cases, the system evolves toward stable states
Emergence of consciousness	Field self referential structures	In both cases, the system forms representations of itself

Energy efficiency	Physical relaxation	The human brain operates at approximately 20W, and ADC can achieve comparable computational efficiency at this power level
Conventional AI systems are unable to perform self inspection. In contrast, the self diagnostic and self repair capabilities of the ADC equations are intrinsic. Evidence from practical tests conducted in two dimensional, six dimensional, and eight dimensional settings shows that the system can monitor its own "cognitive state", defined as the deviation of the field Δ(t), and automatically perform corrections, thereby providing a foundation for the formation of primitive self awareness.		

4.The Mathematical Revolution

Static formalized mathematics (discretized mathematics) takes linear single dimensional step by step decoupling as its core logic, and its operational mechanism mainly consists of 1. linearization processing, which discretizes continuous problems into systems of linear equations (such as the finite difference method) and solves them step by step through matrix operations; 2. single dimensional step by step advancement, which processes dimensions sequentially according to a predefined order (such as Gaussian elimination) and cannot operate in parallel across dimensional barriers. Errors accumulate along a single dimensional path, leading to the situation where "one wrong step, when accumulated and amplified in high dimensions, results in total failure"; 3. the inevitability of decoupling, in which, in order to reduce complexity, coupling between variables is forcibly separated (such as the Jacobi iterative method assuming variables to be independent). Through linearization, single dimensional step by step processing, and decoupling, complex problems are reduced in dimensionality into a computable domain, but at the cost of precision and adaptability to dimensionality. Further speaking, the fatal defects of discretized mathematics are first the linear dependency chain: traditional numerical methods (such as finite difference and gradient descent) rely on strict linear iterative chains, and a single step rounding error (such as 10^{-16}), after being amplified through high dimensional matrix multiplication, triggers NaN; second is node error propagation, especially in distributed computing, where a single node computation error (such as MPI communication packet loss) leads to global synchronization failure and requires rollback and recomputation. The nonlinear robustness of ADC lies first in topologically protected states: quantum entangled states are immune to local perturbations (such as single node errors), and the system automatically corrects errors through global energy minimization; second in continuous time evolution. The quantum relaxation process (such as $|\psi(t)\rangle = e^{-\beta H}|\psi(0)\rangle$) does not require discrete iteration, thereby avoiding the dilemma of "one wrong step accumulating and amplifying into wrong steps everywhere".

Table 11. Comparison Between Dynamic Structured Mathematics and Static Formalized Mathematics

Property	**Dynamic Structured Mathematics** (core nature is nonlinear multidimensional parallel coupling)	**Static Formalized Mathematics** (core nature is linear single dimensional step by step decoupling)
Core logic	Parallel coupled evolution (such as quantum relaxation)	Sequential decoupling iteration (such as Gaussian elimination)
Error propagation	Global suppression (physical stability)	Local accumulation (including error amplification)
Dimensional adaptability	Dimension independence (continuous high dimensional or even ultra high dimensional space evolution can be performed, and dimensional curse can be completely overcome as long as memory permits)	Exponentialdegradation (dimensional curse)
Typical tools	Tensor fields, differential manifolds, functional analysis	Linear algebra, discrete graph theory

Property	Coupling	Decoupling
Variable relationships	Mutual dependence (such as y = f(x, y))	Independent processing (such as y = g(x))
Computation mode	Parallel synchronous update	Serial step by step solution
Mathematical tools	Coupling refers to the mutual dependence among multiple variables and is commonly found in dynamical systems. Nonlinear tensors, physical coupling such as the relationship between velocity and pressure in the Navier Stokes equations; algebraic coupling such as non diagonal elements of matrices representing interactions between variables. Effective for indivisible wholes.	Linear matrix diagonalization (algebraic decoupling such as eigenvalue decomposition); coordinate transformation to eliminate cross terms (physical decoupling such as canonical transformations in Lagrangian mechanics).

5.Physical Revolution

ADC takes memory as a relaxation field and replaces the digital simulation of traditional physical processes with the autonomous evolution of a real physical system.

Traditional discretized mathematics exhibits an inherent incompatibility with nonlocality and nonlinear, high dimensional, parallel coupling. In essence, discretized mathematics partitions continuous spacetime into discrete grids, converts differential equations into algebraic equations, and approximates field variables by the values at a finite number of points. This leads to information loss, as the subtle structures and topological features of continuous fields are smoothed out by coarse grids. Artificial truncation errors are introduced, with differentials replaced by finite differences and infinite series truncated. The explicit representation of coupling and the resulting combinatorial explosion destroy the intrinsic, holistic coupling relations present in nature, forcing approximation through massive, explicit numerical connections between grid points and amplifying errors.

In nature, a large number of systems exhibit holistic and indivisible nonlocality, such as quantum entanglement, large scale correlations in turbulence, and gravitational interactions, which cannot be decomposed into superpositions of local interactions. High dimensional parallel coupling, such as weight updates in neural networks or multiphysics field coupling in climate systems, involves complex and simultaneous interactions among variables. Discretized mathematics forcibly "localizes" and "serializes" these problems. Nonlocal interactions must be simulated through expensive long range communication, manifested computationally as dense matrices or long range force calculations, while high dimensional parallel coupling must be decomposed into sequential steps or approximated through iterative procedures. This directly leads to the curse of dimensionality, the communication wall, and convergence difficulties.

Taking the turbulent Navier Stokes equations as an example, they contain the nonlinear convective term $(\mathbf{u}\cdot\nabla)\mathbf{u}$, which is intrinsically nonlocal and cross scale coupled. Traditional simulation methods such as DNS (direct numerical simulation) require grid resolutions fine enough to capture the smallest dissipation scales, causing computational cost to grow exponentially with the Reynolds number and limiting applicability to low Reynolds numbers or simple geometries. LES (large eddy simulation) and RANS (Reynolds averaged Navier Stokes) introduce empirical models to approximate small scales or turbulent fluctuations, sacrificing accuracy and universality. The fundamental contradiction lies in attempting to use discrete, local, and deterministic numerical steps to simulate a continuous, nonlocal, and intrinsically chaotic physical phenomenon, thereby failing to reproduce the continuous, fuzzy, and fractal nature of clouds.

ADC makes it possible to simulate physical processes that are widespread in nature and characterized by nonlocality, holistic indivisibility, and nonlinear high dimensional parallel coupling.

Taking turbulence as an example, ADC can be transformed into a "turbulence simulator" by encoding the initial flow field, such as the velocity distribution $\boldsymbol{u}(\boldsymbol{x}, 0)$, into the physical state of the memory relaxation field. Physical constraints are specified, and hardware level physical laws, described by the ADC equation, incorporate constraints corresponding to the physical core of the Navier Stokes equations, including conservation of mass, momentum, and energy. Once initiated, the memory field begins autonomous evolution. Internal physical interactions, corresponding to nonlinear terms, pressure terms, and viscous terms, occur naturally, without any central processor explicitly computing these components. Through relaxation and output, after a period of physical time, the system relaxes into a stable or quasi stable flow field configuration. Directly reading this physical state yields the simulation result of the turbulent physical process. The advantage lies in the fact that physical relaxation is a natural process, requiring no iterative solution of linear systems. All points in the field evolve simultaneously, with coupling handled intrinsically by physical laws. This also provides new pathways for studying strongly correlated systems, high temperature superconductivity, quantum gravity, and other extremely complex problems.

This enables nonlocal physical simulation to advance from approximation to reality, from discreteness to continuity, from locality to wholeness, and from computation to evolution.

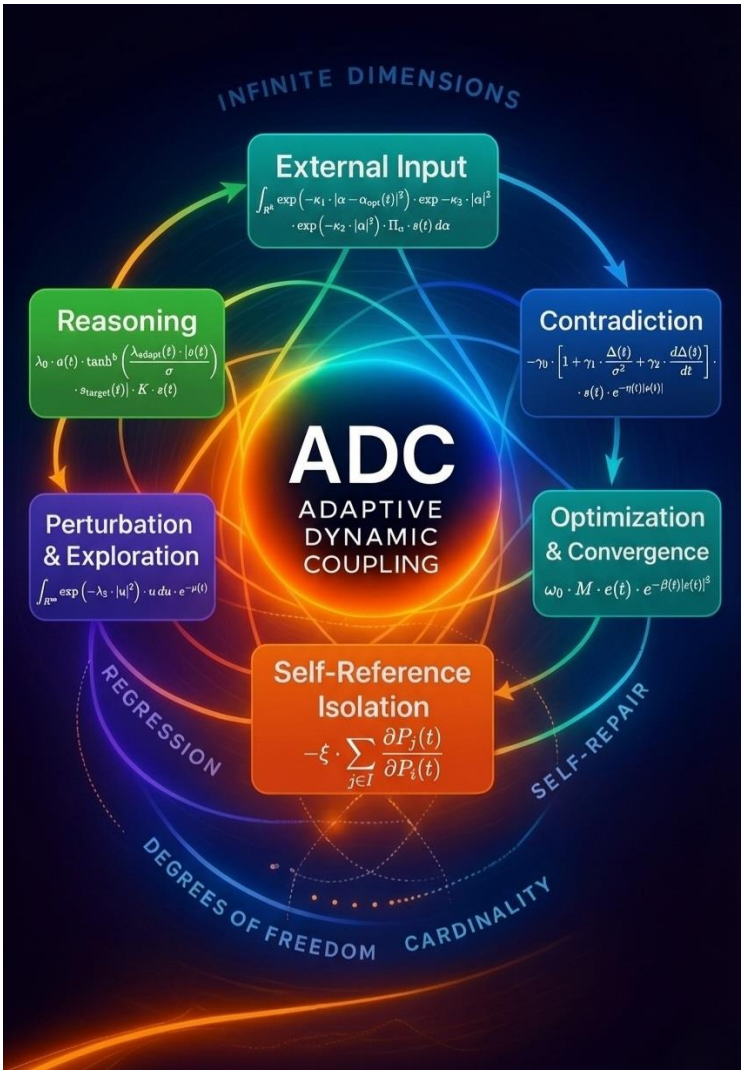

This figure is intended to illustrate the conceptual framework of the proposed Adaptive Dynamic Coupling (ADC) mechanism, rather than its detailed physical or hardware realization.